



Letter

Approaching ^{100}Sn : Structural evolution in $^{98,100}\text{Cd}$ via lifetime measurements



G. Zhang^{a,b,c}, M. Polettini^{b,c,d}, D. Mengoni^{b,c,ld,*}, G. Benzoni^e, Z. Huang^{b,c,f}, M. Górska^g, A. Blazhev^h, L.M. Fraileⁱ, A. Gargano^j, G. De Gregorio^{j,k}, F. Nowacki^l, G. Aggez^g, U. Ahmed^m, O. Aktasⁿ, M. Al-Aqeel^o, B. Alayed^{p,q}, H.M. Albers^g, A. Algora^r, S. Alhomaidhi^{m,g,s,t}, F. Amjad^g, C. Appleton^u, T. Arici^g, M. Armstrong^{h,g}, B.Q. Arnés^v, A. Astier^w, M. Balogh^x, A. Banerjee^g, D. Bazzacco^c, J. Benito Garcíaⁱ, S. Bottoni^{d,e}, P. Boutachkov^g, A. Bracco^{d,e}, A. Bruce^y, D. Brugnara^{b,x}, C. Bruno^u, F. Camera^{d,e}, B. Cederwallⁿ, M. Cicerchia^{b,x}, M.M.R. Chishti^z, A. Corsi^{aa}, M.L. Cortes^x, D. Cox^{ab}, F.C.L. Crespi^{d,e}, B. Dasⁿ, T. Davidson^u, G. de Angelis^x, T. Dickel^g, M. Doncel^{ac}, A. Ertoprakⁿ, A. Esmaylzadeh^h, L. Gaffney^p, F. Galtarossa^c, E.R. Gamba^{d,e}, J. Garbe^h, D. Genna^{d,e}, J. Gerl^g, A. Goasduff^x, A. Gottardo^x, A. Gozzelino^x, T. Grahn^{ad}, J. Ha^{b,c}, E. Haettner^g, O. Hall^u, L. Harkness-Brennan^p, H. Heggen^g, C. Hornung^g, Y. Hrabar^{ab}, S.P. Hu^{ac,af}, N. Hubbard^{m,g,t}, K.E. Ide^m, A. Illana^{ad}, S. Jazrawi^z, P.R. John^m, J. Jolie^h, C. Jones^y, D. Joss^p, D. Judson^p, V. Karayonchev^h, E. Kazantseva^g, R. Kern^m, G.G. Kiss^{ag}, L. Knafla^h, R. Knöbel^g, I. Kojouharov^g, A. Korgul^{ah}, W. Korten^{aa}, P. Koseoglou^m, D. Kostyleva^g, T. Kurtukian-Nieto^{ai}, G. Kosir^{aj,ak}, N. Kurz^g, I. Kuti^{ag}, M. Labiche^{al}, S.M. Lenzi^{b,c}, S. Leoni^{d,e}, G.-S. Li^{am}, Z. Liu^{an}, M. Llanos Expósitoⁱ, R. Lozeva^w, J.B. Lu^{ao}, M. Luoma^{ad}, G. Mantovani^{b,x}, T. Marchi^x, M. Mazzocco^{b,c}, R. Menegazzo^c, T.J. Mertzimekis^{ap}, M. Mikolajczuk^{ah,g}, B. Million^e, A.K. Mistry^{m,g,t}, I. Mukha^g, E. Nacher^r, D.R. Napoli^x, B.S. Nara Singh^{aq}, S.E.A. Orrigo^r, R.D. Page^p, P. Papadakis^{al}, G. Pasqualato^{b,c}, J. Pllumaj^{x,ar}, S. Pelonis^{ap}, R.M. Pérez Vidal^{r,x}, C.M. Petrache^w, J. Petrovicⁿ, N. Pietralla^m, S. Pietri^g, S. Pigliapoco^{b,c}, Zs. Podolyák^z, C. Porzio^{d,e}, A. Raggio^{ad}, F. Recchia^{b,c}, P.H. Regan^{z,as}, J.M. Régis^h, P. Reiter^h, K. Rezyunkina^c, E. Rocco^g, J. Rodriguez Muriasⁱ, H. Rösch^g, P. Roy^g, B. Rubio^r, M. Rudigier^m, P. Ruotsalainen^{ad}, E. Sahin^{m,g,t}, L.G. Sarmiento^{ab}, M.-M. Satrazani^p, H. Schaffner^g, Ch. Scheidenberger^g, L. Sexton^u, A. Sharma^g, M. Siciliano^{at}, J. Simpson^{al}, J. Smallcombe^p, P. Söderström^{au}, D. Sohler^{ag}, A. Soodⁿ, F. Soramel^{b,c}, B.-H. Sun^{am}, H.B. Sun^{av,aw}, A. Sveczer^{ag}, N. Szegedi^{ag}, Y.K. Tanaka^g, J.J. Valiente-Dobón^x, P. Vasileiou^{ap}, J. Vesic^{aj}, M. von Tresckow^m, L. Waring^p, H. Watanabe^{am,ay}, H. Weick^g, V. Werner^{mt}, J. Wiederhold^m, O. Wieland^e, K. Wimmer^{ax}, H.-J. Wollersheim^g, P. Woods^u, J. Wu^{az}, A. Yaneva^{h,g}, I. Zanon^x, J. Zhao^g, H.Q. Zhang^{ba}, G.L. Zhang^{am}, K.K. Zheng^w, L.H. Zhu^{am}, R. Zidarova^m, S. Ziliani^{d,e}, A. Zyriliou^{ap}

^a Sino-French Institute of Nuclear Engineering and Technology, Sun Yat-Sen University, Zhuhai 519082, Guangdong, China

^b Università degli Studi di Padova, Padova 35131, Italy

^c INFN Sezione di Padova, Padova 35131, Italy

^d Università degli Studi di Milano, Milano 20133, Italy

^e INFN Sezione di Milano, Milano 20133, Italy

^f School of Radiation Medicine and Protection, Collaborative Innovation Center of Radiological Medicine of Jiangsu, Soochow 215123, China

^g GSI Helmholtzzentrum für Schwerionenforschung, Darmstadt 64291, Germany

* Corresponding author.

E-mail address: daniele.mengoni@unipd.it (D. Mengoni).

<https://doi.org/10.1016/j.physletb.2025.139378>

Received 8 September 2024; Received in revised form 28 February 2025; Accepted 4 March 2025

Available online 7 March 2025

0370-2693/© 2025 The Author(s). Published by Elsevier B.V. Funded by SCOAP³. This is an open access article under the CC BY license (<http://creativecommons.org/licenses/by/4.0/>).

- ^h Institut für Kernphysik, Universität zu Köln, Cologne 50937, Germany
- ⁱ Grupo de Física Nuclear and IPARCOS, Universidad Complutense de Madrid, Madrid E-28040, Spain
- ^j INFN Sezione di Napoli, Napoli I-80126, Italy
- ^k Università degli Studi della Campania, Caserta 81100, Italy
- ^l Université de Strasbourg, IPHC, Strasbourg 67037, France
- ^m Institut für Kernphysik, Technische Universität Darmstadt, Darmstadt 64289, Germany
- ⁿ Department of Physics, KTH Royal Institute of Technology, Stockholm SE-10691, Sweden
- ^o Imam Mohammad Ibn Saud Islamic University, Riyadh, Saudi Arabia
- ^p Department of Physics, Oliver Lodge Laboratory, University of Liverpool, Liverpool L69 7ZE, UK
- ^q Ar Rass College of Sciences and Arts, Qassim University, Quassim, Saudi Arabia
- ^r Instituto de Física Corpuscular, CSIC-Universidad de Valencia, Valencia E-46071, Spain
- ^s King Abdulaziz City for Science and Technology (KACST), Riyadh 11442, Saudi Arabia
- ^t Helmholtz Forschungsakademie Hessen für FAIR (HFHF), Darmstadt 64289, Germany
- ^u School of Physics and Astronomy, University of Edinburgh, Edinburgh H9 3FD, UK
- ^v Laboratorio de Radiaciones Ionizantes, Universidad de Salamanca, Salamanca 37008, Spain
- ^w Université Paris-Saclay, IJCLab, CNRS/IN2P3, Orsay F-91405, France
- ^x INFN Laboratori Nazionali di Legnaro, Legnaro 35020, Italy
- ^y School of Computing Engineering and Mathematics, University of Brighton, Brighton BN2 4AT, UK
- ^z Department of Physics, University of Surrey, Surrey GU2 7XH, UK
- ^{aa} IRFU, CEA, Université Paris-Saclay, 91191 Gif-sur-Yvette, France
- ^{ab} Department of Physics, Lund University, Lund SE-221 00, Sweden
- ^{ac} Department of Physics, University of Stockholm, Stockholm SE-106 91, Sweden
- ^{ad} University of Jyväskylä, Jyväskylä 40014, Finland
- ^{ae} Institute for Advanced Study in Nuclear Energy and Safety, Shenzhen University, 518060 Shenzhen, China
- ^{af} Shenzhen Key Laboratory of Research and Manufacture of High Purity Germanium Materials and Detectors, Shenzhen University, 518060 Shenzhen, China
- ^{ag} HUN-REN Institute for Nuclear Research (HUN-REN ATOMKI), Debrecen 4001, Hungary
- ^{ah} Faculty of Physics, Warsaw University, Warsaw PL-02-093, Poland
- ^{ai} CENBG, Université de Bordeaux-UMR 5797 CNRS/IN2P3, Gradignan 33175, France
- ^{aj} Jozef Stefan Institute, Ljubljana 1000, Slovenia
- ^{ak} Faculty of Mathematics and Physics, University of Ljubljana, Ljubljana 1000, Slovenia
- ^{al} STFC Daresbury Laboratory, Daresbury WA4 4AD, UK
- ^{am} School of Physics, Beihang University, Beijing, 100191, China
- ^{an} Institute of Modern Physics, Chinese Academy of Sciences, China
- ^{ao} College of Physics, Jilin University, Changchun, 130012, China
- ^{ap} Department of Physics, University of Athens, Zografou Campus, 15784 Athens, Attiki, Greece
- ^{aq} School of Computing, Engineering and Physical Sciences, University of the West of Scotland, Paisley PA1 2BE, UK
- ^{ar} Dipartimento di Fisica e Scienze della Terra, Università di Ferrara, Ferrara 44122, Italy
- ^{as} National Physical Laboratory, Teddington TW11 0LW, UK
- ^{at} Physics Division, Argonne National Laboratory, Argonne IL 60439, USA
- ^{au} ELI-NP and IFIN-HH, Magurele 077125, Romania
- ^{av} Shenzhen Key Laboratory of Advanced Thin Films and Applications, College of Physics and Energy, Shenzhen University, Shenzhen 518060, China
- ^{aw} Key Laboratory of Optoelectronic Devices and Systems, College of Optoelectronic Engineering, Shenzhen University, Shenzhen 518060, China
- ^{ax} Instituto de Estructura de la Materia, Consejo Superior de Investigaciones Científicas, Madrid 28006, Spain
- ^{ay} RIKEN Nishina Center, 2-1 Hirosawa, 351-0198, Wako, Saitama, Japan
- ^{az} Facility for Rare Isotope Beams, Michigan State University, East Lansing, MI 48824, USA
- ^{ba} China Institute of Atomic Energy, 102413 Beijing, China

ARTICLE INFO

Editor: B. Blank

Keywords:

Nuclear structure
Lifetime measurement
Gamma-ray spectroscopy
Radioactive beams

ABSTRACT

The lifetimes of low-lying excited states below the 8^+ seniority isomer were directly measured using fast timing detectors in the neutron-deficient isotopes $^{98,100}\text{Cd}$. This experiment was conducted with the DEcay SPECTroscopy (DESPEC) setup at GSI, where the ions of interest were produced via a fragmentation reaction and identified using the FRagment Separator (FRS) before being implanted in the AIDA active stopper system, and the γ rays emitted during the de-excitation of isomeric states were detected by the LaBr₃ FATIMA Array. The newly deduced values for the reduced transition probabilities were compared with shell-model calculations using different interactions and effective charges. The results indicate that, while ^{98}Cd aligns well with a seniority scheme description, in ^{100}Cd the transition strengths among low-lying states are not fully reproduced, and the nature of these states remains an open problem within the present theoretical description. Ultimately, a key element in the description of this region, crucial for nuclear physics and astrophysics, appears to be the proton-neutron term of the nuclear effective interaction.

1. Introduction

The characteristics of various composite quantum systems that serve as fundamental building blocks of matter, such as hadrons, atomic nuclei, atoms, and molecules, are largely determined by energy gaps emerging between quantum states. These energy gaps originate from the interactions between their fermionic constituents. Notably, in the context of atomic nuclei, these energy gaps are evident through the presence of specific stable isotopes, that exhibit remarkable resilience against particle separation and internal excitation.

The nuclear structure of doubly magic nuclei such as ^{100}Sn and its neighbors has gained considerable attention from both experimental and

theoretical sides. This interest arises due to the unique insights which provides for testing the nuclear shell model and its relevance to the astrophysical rapid-proton capture process [1]. However, ^{100}Sn is distant from the β stability line, leading to limited experimental data on its spectroscopic properties. In particular, there is a lack of experimental information regarding the excited states of ^{100}Sn , key for understanding the $N = Z = 50$ shell gap and for benchmarking structural models in the $A \approx 100$ proton-rich nuclei region. The extent of the neutron shell gap with $N = 50$ has hitherto been inferred through the exploration of core-excited states within lighter neighboring nuclei [2–4]. Similarly, deductions have been drawn for the proton shell closure with $Z = 50$

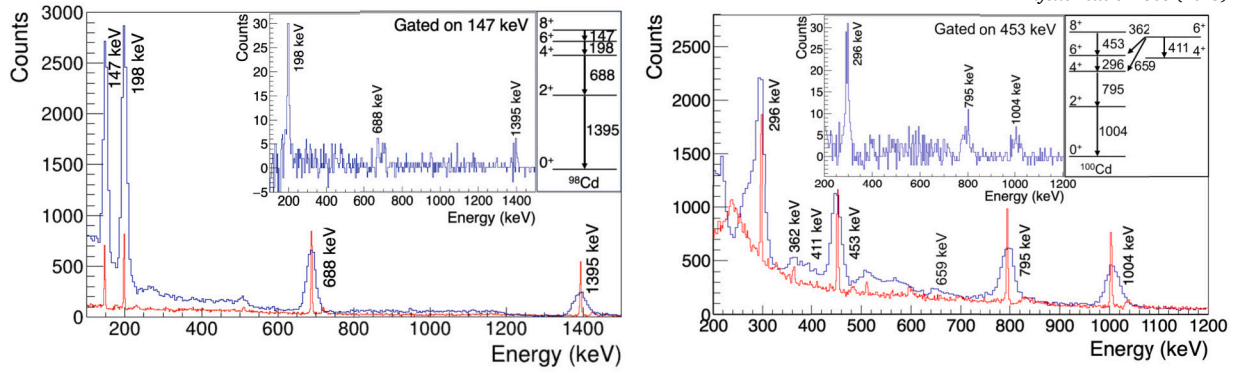


Fig. 1. Gamma-ray energy spectrum obtained for γ -ray transitions with PID condition for $\text{LaBr}_3(\text{Ce})$ (blue) and the HPGe detectors (red) for $^{98,100}\text{Cd}$, on the left and right side, respectively. In the insets, 147-keV (453-keV) gated $\text{LaBr}_3(\text{Ce})$ spectrum for ^{98}Cd (^{100}Cd) and respective level schemes. Features in the $\text{LaBr}_3(\text{Ce})$ spectra that do not appear in the HPGe spectra are primarily due to excitations of the $\text{LaBr}_3(\text{Ce})$ detectors.

based on the examination of the Gamow-Teller (GT) decay strength distribution within ^{100}Sn [5,6].

Cd isotopes, two proton holes away from Sn, show a similar trend in spectroscopic information and reduced transition probabilities and are therefore instrumental for such studies. An extensive set of experimental data has been collected over the years covering low- and high-spin states along the whole isotopic chain from $N=50$ to $N=82$ [1], typically using fusion-evaporation experiments and isomer-delayed γ -ray spectroscopy. In particular the $N=Z$ nucleus ^{96}Cd is, so far, the most neutron-deficient $Z = 48$ isotope for which information about excited states is available [7,8]. However, the information on lifetimes in the neutron-deficient light Cd isotopes is more scarce. Lifetimes in the ps range have been determined for high-spin states in ^{102}Cd [9] and its first 2^+ state as reported in Refs. [10,11]. The doublet of 4^+ , 6^+ , 8^+ states indicates the competition of $g_{9/2}$ proton hole and neutron pair breaking at similar energies. A 2^+ state was proposed at 1930(20) keV in a two-neutron removal knock-out reaction by Corsi et al. (Ref. [12]). In ^{104}Cd , the 2^+ and 4^+ states have been measured by Boelaert et al. [11], whilst Müller et al. [13] determined lifetimes of the high-spin states. The results also shed new light on the way collective effects gradually build up from the underlying proton and neutron contributions and the associated coherence. Using the Recoil Distance Doppler Shift (RDDS) technique, lifetimes of 2^+ and 4^+ states in even-mass $^{102-108}\text{Cd}$ were obtained [14]. The results align well with Ref. [15] where multiple coexisting shapes are claimed to mix potentially strongly affecting the transition probabilities.

Cd nuclei have been studied using shell-model calculations for the lighter nuclides [9–11,13,16–22] starting from cores of either ^{88}Sr or ^{90}Zr . Residual effective interactions are often determined phenomenologically by fit to the data, or by adjusting the monopole terms to a microscopically derived G matrix. Good agreement is found for the level structure and for the $B(E2)$ values of low-lying yrast states for light $^{102-108}\text{Cd}$ isotopes, yet discrepancies exist, notably due to the presence of intruding states, with decreasing energy when approaching mid-shell [15].

Interacting boson model (IBM) [13,23–33] calculations were also used to interpret the light Cd systems. It allowed a simultaneous treatment of the vibrational, the rotational, and the non-collective single-particle degrees of freedom, providing a description of low and high-spin states.

In the present work, we report on an in-beam γ -ray spectroscopy measurements on $^{98,100}\text{Cd}$ populated in fragmentation reactions and subsequently implanted in an active catcher, in order to extract lifetime information on excited states below the isomers and infer to structure properties of the Cd isotopes in the context of the doubly magic ^{100}Sn region.

2. Experimental details and results

The experiment was performed at the GSI accelerator facility, producing nuclei of interest via fragmentation reactions induced by an 840 A MeV ^{124}Xe beam on a 6.333 g/cm² thick ^9Be target. The FRagment Separator (FRS) [34] employing the $B\rho$ - ΔE - $B\rho$ method was used for ion selection and transmission. Within a 10-day beamtime, around one million ^{98}Cd and 7 million ^{100}Cd ions were identified by the FRS and delivered to the final focal plane of the FRS, in which the DE-SPEC [35] (Decay SPECTroscopy) experimental setup was installed for decay spectroscopy measurements. Ions were identified using the ToF- $B\rho$ - ΔE method, measuring their mass number over ionic charge (A/Q) and atomic number Z , with a relative resolution of 0.3% and 0.14%, respectively. The ions of interest were implanted in an active stopper, AIDA (Advanced Implantation Detector Array) [36], consisting of two layers of highly-pixelated DSSDs (Double-Sided Silicon Strip Detectors), covering the full focal plane of 24×8 cm². Two plastic scintillators (β Plastic) were placed upstream and downstream the AIDA stack for time reference. The γ rays deexciting the long-lived isomeric states in $^{98,100}\text{Cd}$ were measured by a hybrid detector array, comprising 4 EUROBALL Cluster germanium detectors [37] and 36 $\text{LaBr}_3(\text{Ce})$ detectors (FATIMA - FAST TIMing Array) [38], surrounding the implantation region. The global synchronization of the various DESPEC subsystems was achieved using a White Rabbit timing [39] which is driven by a 125 MHz clock, and with a timestamp accuracy of ~ 1 ns [35].

Given the ion identification in FRS, it is possible to search for the presence of isomers by measuring their decay as a function of ion- γ or γ - γ time difference. The established isomers in $^{98,100}\text{Cd}$ have served as benchmarks to validate the experimental method. In the current work, a lifetime of 91(5) ns for 8^+ isomer in ^{100}Cd is obtained using ion- γ correlation in the absence of upper feeder, which is consistent with the measured average value from Refs. [40–42]. The lifetime of 6^+ isomer in ^{98}Cd is measured using γ - γ time difference to be 21(1) ns, compatible with the average literature value from Ref. [18,43], i.e., ≤ 29 ns and 19(3) ns, respectively. The data quality is illustrated in Fig. 1, showing the γ -ray spectra for $\text{LaBr}_3(\text{Ce})$ (blue) and the HPGe detectors (red) gated on the Particle Identification (PID) for $^{98,100}\text{Cd}$, respectively. The insets display the 147-keV (453-keV) gated $\text{LaBr}_3(\text{Ce})$ spectrum for ^{98}Cd (^{100}Cd) and the corresponding level schemes.

The FATIMA scintillator detectors were used to measure directly the decay curve with respect to a reference transition time. Gamma-gamma time difference spectra were generated using double energy conditions of ± 20 keV for the start and stop transition, respectively. To this aim, detectors were energy calibrated and time aligned using the calibration sources and an intrinsic time resolution of ~ 320 ps was obtained [35, 38].

The lifetime of the 4^+ state in $^{98,100}\text{Cd}$ was deduced using the Generalized Centroid Difference (GCD) method [44,45]. Assuming no back-

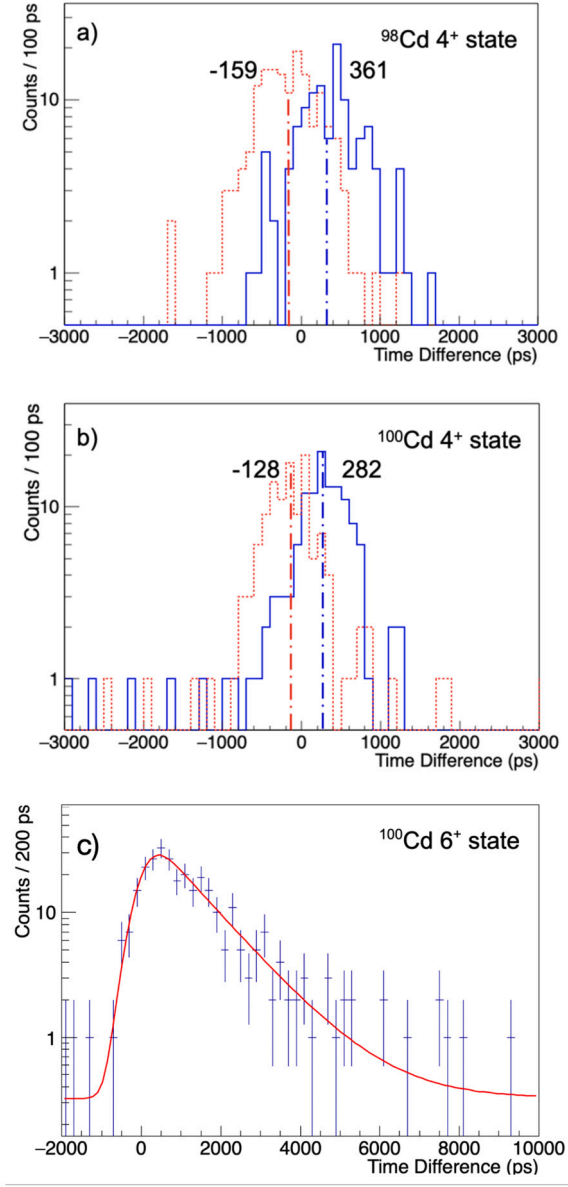


Fig. 2. Delayed (red, dashed) and antidelayed (blue, continuous) time distribution for 4^+ state, 198- and 688-keV in ^{98}Cd (panel a), 296- and 795- transitions ^{100}Cd (panel b). Lifetime of the 6^+ state in ^{100}Cd is fitted with the deconvolution method on a time distribution between 296- and 453-keV transitions (panel c). An energy window of ± 20 keV was used in the gamma-ray coincidence matrix.

ground contribution, the centroid difference ΔC for a coincident γ -ray pair is directly related to the intermediate level τ , following the relation:

$$\Delta C = PRD(\Delta E_\gamma) + 2\tau \quad (1)$$

where, ΔE_γ is the energy difference between the feeding and the decaying γ rays of the level and PRD is the Prompt Response Difference for delayed and anti-delayed time distributions. The calibration of the PRD as a function of the energy is based on the data acquired with an ^{152}Eu source and gives a correction for the time walk.

The delayed and anti-delayed time distributions obtained for the yrast 4^+ state in $^{98,100}\text{Cd}$ are shown in Fig. 2 panel a) and b), from which the centroid shifts were obtained.

A correction t_{corr} for the time-correlated Compton background underneath the γ -ray feeder and decay peak was applied to the measured centroid C of the delayed and anti-delayed distribution [46]:

Table 1

Experimental lifetimes obtained for ^{98}Cd (upper part) and ^{100}Cd (lower part). Value marked with “*” is taken from Refs. [17,18,43].

Isotope	I_γ^*	τ
^{98}Cd	8_1^+	222(23)* ns
	6_1^+	21(1) ns
	4_1^+	58(27) ps
	2_1^+	—
^{100}Cd	8_1^+	91(5) ns
	6_1^+	1.2(1) ns
	4_1^+	36(25) ps
	2_1^+	—

$$t_{corr} = \frac{C - C_{bg}}{P/B} \quad (2)$$

where, C_{bg} is the time response of the background and P/B is the peak-to-background ratio of the considered γ ray. Due to the energy-dependent time-walk effect, the C_{bg} was generated using energy conditions in different background regions, surrounding the peak of interest in the E_γ (feeder)- E_γ (decay) matrix. The P/B ratio was derived from the E_γ spectrum in Fig. 1. Upon background assessment, t_{corr} was estimated at (14 ± 11) ps and (0.4 ± 10) ps for delayed and anti-delayed distributions, respectively, yielding a background-corrected ΔC of $-506(50)$ ps. Considering the PRD value of $-623(20)$ ps, the lifetime of the 4^+ state in ^{98}Cd was determined to be 58(27) ps. The lifetime of the 4_1^+ state in ^{100}Cd was extracted using the same method for the centroid shift and background correction, and it is calculated to be 36(25) ps.

The lifetime τ of the 6_1^+ state in ^{100}Cd was measured for the first time in the current experiment. The value of 1.2(1) ns was obtained with a fit of the delay response (exponential function) deconvoluted from the prompt (Gaussian) one. Fig. 2 panel c) shows the spectrum with the deconvolution fitting. The corresponding value for the reduced transition probabilities $B(E2)$ is calculated to be $290(30) e^2 fm^4$, accounting for the expected internal conversion coefficient of 0.0339(5) [47]. All the newly observed lifetimes in $^{98,100}\text{Cd}$ are summarized in Table 1.

3. Discussion

In the current work, the lifetimes for the 4_1^+ state in ^{98}Cd and 4_1^+ , 6_1^+ states in ^{100}Cd have been measured for the first time, and the respective $B(E2)$ values have been obtained. Such measurements give access to nuclear wave functions in the most neutron-deficient systems in the Cd isotopic chain, being only two neutrons away from the expected proton drip line. The $B(E2; 4_1^+ \rightarrow 2_1^+)$ in ^{98}Cd well aligns with the existing trend in $N=50$ isobaric chain, and, therefore, fits well in a seniority scheme interpretation, see Fig.3 in Ref. [48]. The $B(E2; 4_1^+ \rightarrow 2_1^+)$ values in $^{98,100}\text{Cd}$ are the smallest among the neighboring $^{102-114}\text{Cd}$ isotopes, and, despite the large experimental uncertainties, the data seem to indicate a decrease approaching $N=50$, see also panel b) in Fig. 8 of Ref. [14].

The shell model represents the most effective theoretical approach for a precise description of the nuclear phenomena in this mass region. Refined calculations at the forefront of theory have therefore been conducted to interpret the nature of the measured states and their consequential impact on understanding the Cd systems.

3.1. Calculations for ^{98}Cd

In the case of ^{98}Cd a valence space spanned by the $0f_{5/2}$, $1p_{3/2}$, $1p_{1/2}$, $0g_{9/2}$ orbitals outside ^{56}Ni was considered. The proton single-particle energies (SPEs) are taken from the experimental spectrum of ^{57}Cu , except for the $0g_{9/2}$ orbital that is not yet observed, and was estimated to be 3.2 MeV with respect to the gs state of ^{57}Cu . In the adopted space, only protons are active, while neutrons, which completely fill the

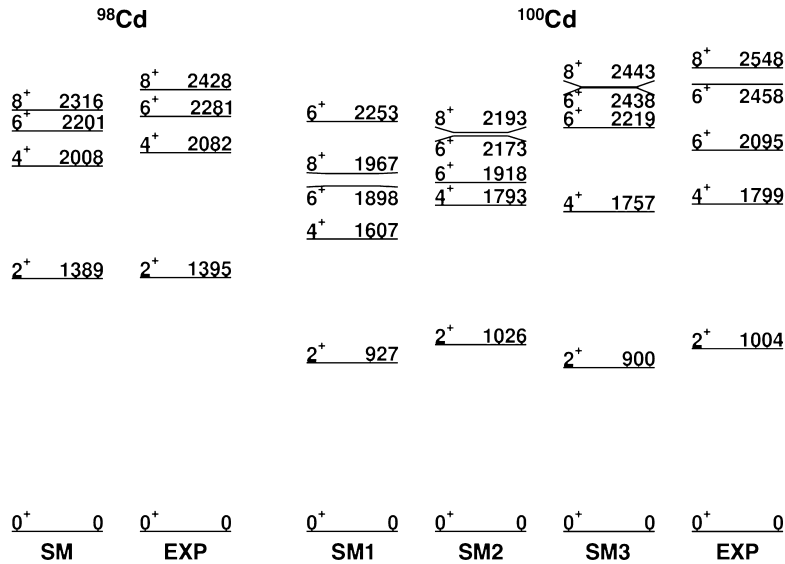


Fig. 3. Experimentally measured level scheme compared to excitation energies obtained from shell-model calculations. SM calculations uses an effective interaction derived from the CD-Bonn NN potential and a model space spanning $0f_{5/2}, 1p_{3/2}, 1p_{1/2}, 0g_{9/2}$ outside a ^{56}Ni core, for both protons and neutrons. Starting from the same bare potential, SM1 includes an identical proton valence space than SM but $0g_{7/2}, 1d_{5/2}, 1d_{3/2}, 2s_{1/2}, 0h_{11/2}$ orbitals for neutrons, SM2 valence space extends over $\pi(1p_{1/2}0g_{1d_{5/2}})$ and $\nu(0g_{7/2}1d_{2s}0h_{11/2})$ orbitals and SM3 uses the $\pi\nu(0g_{1d_{2s}})$ valence space outside ^{80}Zr . All level energies are well reproduced by theory in the ^{98}Cd case, while diverse cores and valence spaces were considered for ^{100}Cd , reaching the best agreement with the SM3 model (see text for further details).

Table 2

Experimental and calculated $B(E2)$ strengths ($e^2 \text{fm}^4$) in ^{98}Cd (top) and ^{100}Cd (bottom). Values marked with “*” is taken from Refs. [40,43].

Isotope	$I_i^\pi \rightarrow I_f^\pi$	$B(E2)_{Exp}$	$B(E2)_{SM}$		
			SM1	SM2	SM3
^{98}Cd	$8^+ \rightarrow 6^+$	39(4)*		51	
	$6^+ \rightarrow 4^+$	110(5)		126	
	$4^+ \rightarrow 2^+$	98(50)		179	
	$2^+ \rightarrow 0^+$	-		153	
^{100}Cd	$8^+ \rightarrow 6^+$	60(30)*	0.004	94	58
	$8^+ \rightarrow 6^+$	0.42(5)*	57	2	0.06
	$6^+ \rightarrow 4^+$	290(30)	170	107	283
	$4^+ \rightarrow 2^+$	71(40)	267	575	574
	$2^+ \rightarrow 0^+$	-	201	476	391

28 – 50 shell, simply affect the proton effective SPEs. The Two-Body Matrix Elements (TBMEs) of the residual effective interaction are obtained within the many-body perturbation theory starting from the CD-Bonn NN potential as described in Ref. [49], with the Coulomb interaction coherently taken into account. The $E2$ transition strengths are calculated using microscopic effective charges derived consistently with the effective Hamiltonian [50]. Then, the obtained proton effective charges depend on the involved orbitals, ranging from 1.2 to 1.6 e.

The calculated excitation energies and $B(E2)$ values are reported in Fig. 3 and Table 2, respectively, and compared with the present experimental values and data already available in the literature [51]. All level energies are well reproduced by theory, with the largest discrepancy found for the 8^+ state which is predicted to lie about 100 keV below the observed one.

As regards the $B(E2)$ values, the agreement between theory and experiment is very good for the $8^+ \rightarrow 6^+$ and $6^+ \rightarrow 4^+$ transitions, and the $B(E2, 4^+ \rightarrow 2^+)$ locates within the measured error bars, close to the upper limit.

It is worth mentioning that the same shell-model results for ^{98}Cd were already presented in Ref. [48], aiming at studying the seniority conservation in the $N = 50$ isotones. The conclusion of this paper was that seniority is largely conserved along the $N = 50$ yrast states from ^{90}Zr to ^{98}Cd , corresponding to the filling of the proton $0g_{9/2}$ orbital. Slight deviations between theory and experiment were only observed for the $4^+ \rightarrow 2^+$ transitions in ^{94}Ru and ^{96}Pd , which were attributed to

some inaccuracies in the description of the 4^+ state in these two nuclei, probably originating from limitations of the adopted model space.

3.2. Calculations for ^{100}Cd and comparison among different models

On these grounds, the calculations were extended to ^{100}Cd by taking as valence space for the two additional neutrons the $0g_{7/2}, 1d_{5/2}, 1d_{3/2}, 2s_{1/2}, 0h_{11/2}$ orbitals of the 50 – 82 shell. The adopted effective shell-model Hamiltonian, referred to the ^{78}Ni core, is described in Ref. [52]. In this case the SPEs are also microscopically derived since no experimental data are available for systems with one-valence nucleon outside ^{78}Ni . As in the calculations of the $B(E2)$ s for ^{98}Cd , microscopic effective charges have been employed, whose values are reported in Ref. [52].

Excitation energies and $B(E2)$ values, referred to as SM1, are reported in Fig. 3 and Table 2, respectively, together with the available experimental data. The agreement between theory and experiment is significantly worse than that obtained for ^{98}Cd . All level energies are underestimated by calculations, discrepancies being particularly relevant, in the order of 0.5 MeV, for the 8^+ state. Deficiencies of our calculations are also testified by their failure to reproduce the experimental $B(E2)$ strengths, which questions the reliability of the predicted wavefunctions. Theory overestimates the $4^+ \rightarrow 2^+$ and $8^+ \rightarrow 6^+$ transitions, while the other two known experimental $B(E2)$ values, namely $B(E2, 6^+ \rightarrow 4^+)$ and $B(E2, 8^+ \rightarrow 6^+)$, are underestimated.

Such deficiencies might originate from the need to employ a larger valence space including proton excitation across the $Z = 50$. It is well established that for light tin isotopes - with few neutrons above the $N = 50$ shell closure - the role of $Z = 50$ cross-shell excitations is crucial to explain the measured quadrupole collectivity of the $B(E2)$ values, as discussed in, e.g., Refs. [53–55]. In order to improve the description of ^{100}Cd , we have employed an effective Hamiltonian derived from the CD-Bonn NN potential, a valence space above ^{88}Sr spanned by the $\pi(1p_{1/2}0g_{1d_{5/2}})$ and $\nu(0g_{7/2}1d_{2s}0h_{11/2})$ orbitals and microscopic effective charges, as in Ref. [54]. The excitation energies and $B(E2)$ strengths are shown in Fig. 3 and Table 2, labeled as SM2. With respect to SM1 results, a more satisfactory agreement between theory and experiment is obtained for the energy spectrum, and the SM2 calculations also lead to significant changes in the $B(E2)$ values. However, an improvement in the description of the $B(E2)$ values is obtained only for the $8^+ \rightarrow 6^+$

Table 3
Proton, neutron, and interference components of the $B(E2)$ in ^{100}Cd (in $e^2 \text{fm}^4$). See text for details.

	$I_i^\pi \rightarrow I_f^\pi$	A_p^2	A_n^2	$2 \times A_p A_n$
SM1	$8^+ \rightarrow 6_2^+$	0.00	0.04	0.02
	$8^+ \rightarrow 6_1^+$	694	23.0	253
	$6^+ \rightarrow 4_1^+$	1431	88.9	713
	$4_2^+ \rightarrow 2_1^+$	11	133	-77
	$4_1^+ \rightarrow 2_1^+$	1470	119	837
SM2	$8^+ \rightarrow 6_2^+$	962	82.4	563
	$8^+ \rightarrow 6_1^+$	24.9	0.42	6.25
	$6^+ \rightarrow 4_1^+$	542	195	651
	$4_2^+ \rightarrow 2_1^+$	5	152	-56
	$4_1^+ \rightarrow 2_1^+$	2681	406	2086

and $8^+ \rightarrow 6_2^+$ transitions, large discrepancies still persisting for the other two available experimental $B(E2)$ values.

To shed light on these results, we have compared the SM1 and SM2 wave functions in terms of the proton and neutron basis states, namely $^{98}\text{Cd}(J_p^\pi) \otimes ^{102}\text{Sn}(J_n^\pi)$. Each state can then be identified with a leading component, even if the decomposition indicates a significant fragmentation of the wave functions for both calculations. In SM1, the ground state is essentially governed by the $^{98}\text{Cd}(0_1^+) \otimes ^{102}\text{Sn}(0_1^+)$ component, while the yrast $J^\pi = 2^+, 4^+, 6^+, 8^+$ states are of proton nature, namely they are dominated by the excited valence proton configuration ($J_p = J^\pi$, $J_n = 0^+$), the 6_2^+ state being characterized by the configuration ($J_p = 0^+$, $J_n = 6^+$) instead. The inclusion of proton cross-shell excitations in SM2 provides an inversion in the structure of the two 6^+ states, and the state characterized by the ($J_p = 0^+$, $J_n = 6^+$) component becomes the yrast one. This change increases the proton component of the $8^+ \rightarrow 6_2^+$ transition making it the favorite one compared to the $8^+ \rightarrow 6_1^+$ transition, as experimentally observed. This is shown in Table 3, where the proton, neutron and proton-neutron components of the $B(E2)$ are reported, as expressed by:

$$B(E2; J_i \rightarrow J_f) = \frac{1}{(2J_i + 1)} (A_p^2 + A_n^2 + 2A_p A_n) \quad (3)$$

In Eq. (3), A_p (A_n) is the reduced matrix element for the proton (neutron) contribution to the transition.

As for the other states, a larger admixture between proton and neutron excitations is predicted by SM2, but their nature does not change substantially with respect to the SM1 predictions. In particular, the 2^+ and 4^+ states are still dominated by the valence proton $J_p = 2^+$, $J_n = 0^+$ and $J_p = 4^+$, $J_n = 0^+$ component, respectively. The analysis of the $B(E2; 4^+ \rightarrow 2^+)$ and $B(E2; 6_1^+ \rightarrow 4^+)$ in terms of the proton and neutron contributions is given in Table 3. The proton cross-shell excitations do not improve the agreement with experiment - on the contrary they make it worse - which may indicate the need to include also $N = 50$ neutron cross-shell excitations. In this line, we have extended the calculations with the effective interaction of Ref. [8], defined in the $\pi\nu(0g1d2s)$ valence space outside ^{80}Zr . Results are reported in Fig. 3 and Table 2 as SM3. Overall, discrepancies are further reduced with respect to SM2 for both excitation energies and $B(E2)$ strengths, but we are still unable to explain the transitions involving the 4^+ state.

It appears evident that none of the theoretical calculations presented here are able to consistently describe the experimental values in ^{100}Cd and there remains a discrepancy between the transitions from the 4_1^+ to the 2_1^+ state. Hence, possible factors behind the discrepancies between theoretical and experimental results have been explored. Given the accurate description of ^{98}Cd [48] and ^{104}Sn [56,57], terms of proton-proton and neutron-neutron interactions have been excluded, narrowing down to the proton-neutron interaction along with the proton and neutron shell gap. The proton shell gap was alternatively increased and decreased by 1 MeV, resulting in still inadequate description of experimental data. Considering the limited impact of the shell gap on experimental results, the primary element appears to be the proton-neutron

interaction term. This hypothesis is supported by the presence of a 4_2^+ state with an excitation energy quite close to that of the yrast one and a quite small predicted transition strength to the 2_1^+ state ($11 e^2 \text{fm}^4$ for SM2). This small value is due also to the negative sign of the double product term of the $B(E2)$ (see Table 3) evidencing the destructive interference of the proton-neutron interaction. An appropriate proton-neutron interaction could provide more mixing between these two 4^+ states or even lead to their inversion. It is worth noting that results of our calculations for the second 4^+ state are consistent with a mixed symmetry nature [58]. In fact, in addition to the weak $E2$ transition to the 2_1^+ state, we find an intense $M1$ ($1 \mu_N^2$ for SM2) and a weak $E2$ ($3 e^2 \text{fm}^4$ for SM2) transition to the 4_1^+ state, with a possible fully-symmetric character. Some of these states, 1^+_{ms} and 2^+_{ms} , have already been proposed in the Cd isotopic chain [10]. In Ref. [59], the properties of the 4^+_{ms} state in ^{94}Mo have been explained within the sdg-IBM-2 introducing the g-boson, wholly compatible with the present interpretation.

Identifying the effect of proton-neutron term in the interaction appears essential to the understanding of the region, key for both nuclear structure and astrophysics. Future experimental works capable of measuring half-lives and extracting spectroscopic factors in the light neutron-deficient indium isotopes, i.e. ^{100}In , where the contribution is expected to be limpid, are therefore imperative.

4. Conclusions

In the current work, the lifetimes of the 4_1^+ state in ^{98}Cd and 4_1^+ , 6_1^+ states in ^{100}Cd have been directly measured for the first time. The experiment was performed at GSI using the FRS+DESPEC setup, where the ions of interest were populated via fragmentation reactions and implanted in the AIDA active stopper. The lifetimes of excited states below the long-lived isomer were measured using the FATIMA LaBr₃(Ce) array. The newly deduced $B(E2)$ values have been compared with shell model calculations using different interactions and valence spaces.

The results emphasize the importance of core-breaking contributions as well as the relevance of the proton-neutron term in the interaction in the low-lying states and, especially, in the 4^+ state, that provides crucial indications for understanding the nuclear structure in the region. These effects might not have a large impact on the excitation energies, whereas they appear to significantly influence the transition strengths, a key element for the coherent description of these nuclei and the region as a whole.

Declaration of competing interest

The authors declare that they have no known competing financial interests or personal relationships that could have appeared to influence the work reported in this paper.

Acknowledgements

The authors would like to acknowledge the excellent work of the local GSI group as well as the accelerator teams. The results presented here are based on the experiment S496, which was performed at the DESPEC decay station at the GSI, Helmholtzzentrum für Schwerionenforschung, Darmstadt (Germany) in the frame of FAIR Phase-0. Support is acknowledged to INFN. This work was partially supported by (M.S.) the U.S. Department of Energy, Office of Science, Office of Nuclear Physics, under contract number DE-AC02-06CH11357. This work was supported by (R.D.P. and Zs.P.) the United Kingdom Science and Technology Facilities Council through the grants ST/P004598/1, ST/V001027/1 and ST/V001108/1. S.E.A.O. acknowledges the support of the Generalitat Valenciana Grant No. PROMETEO/2019/007 and Spanish MICIN Grant No. PID2019-104714GB-C21. Support by the Spanish funding agency MCIN-AEI 10.13039/501100011033 (FEDER, EU) under grants RTI2018-098868-B-I00 and PID2021-126998OB-I00

is acknowledged. Support by the BMBF-Rahmenprogramm ErUM Verbundprojekt ErUM-FSP T07 grant nos. 05P19PKFNA, 05P21RDFNA, 05P21RDFN1, 05P19RDFN1 is acknowledged by M.L.C., N.H., K.I., P.R.J., P.K., A.K.M., E.S., V.W., J.W. and R.Z., N.H., A.K.M., E.S., and V.W. acknowledge support by the Helmholtz Research Academy Hesse for FAIR (HFHF) and funds for cooperation between TU Darmstadt and GSI. This work was supported by the Swedish Research Council under Grant No. 2019-04880. Support by the STFC under Grants No. ST/G000697/1, No. ST/P005314, and No. ST/P003982/1 and No. ST/P004598/1 and No. ST/V001027/1; and support from the National Measurements System Programmes Unit of the UK's Department for Science, Innovation and Technology (DESIT) J.V. and G.K. want to acknowledge funding by the Slovenian Research and Innovation Agency under grants no: P1-0102, I0-E005. K.G. wants to acknowledge NKFIH support (K147010). This work was partially supported by MCIN/AEI/10.13039/501100011033, Spain with grant PID2020-118265GB-C42, by Generalitat Valenciana, Spain with grant CIAPOS/2021/114 and by the EU FEDER funds. This work was supported by Young Scientists Fund of the National Natural Science Foundation of China (No. 12405144). This work was supported by Guangdong Basic and Applied Basic Research Foundation under Grant No. 2025A1515012112.

Data availability

Data will be made available on request.

References

- [1] T. Faestermann, M. Górška, H. Grawe, Prog. Part. Nucl. Phys. 69 (2013) 85–130, <https://doi.org/10.1016/j.pnpnp.2012.10.002>.
- [2] G. Guastalla, D.D. DiJulio, M. Górška, J. Cederkäll, P. Boutachkov, et al., Phys. Rev. Lett. 110 (2013) 172501, <https://doi.org/10.1103/PhysRevLett.110.172501>.
- [3] V.M. Bader, A. Gade, D. Weisshaar, B.A. Brown, T. Baugher, et al., Phys. Rev. C 88 (2013) 051301, <https://doi.org/10.1103/PhysRevC.88.051301>.
- [4] P. Doornenbal, S. Takeuchi, N. Aoi, M. Matsushita, A. Obertelli, et al., Phys. Rev. C 90 (2014) 061302, <https://doi.org/10.1103/PhysRevC.90.061302>.
- [5] D. Lubos, J. Park, T. Faestermann, R. Gernhäuser, R. Krücken, et al., Phys. Rev. Lett. 122 (2019) 222502, <https://doi.org/10.1103/PhysRevLett.122.222502>.
- [6] C.B. Hinke, M. Böhmer, P. Boutachkov, T. Faestermann, H. Geissel, et al., Nature 486 (7403) (2012) 341–345, <https://doi.org/10.1038/nature11116> and Supplemental Material.
- [7] P.J. Davies, J. Park, H. Grawe, R. Wadsworth, R. Gernhäuser, et al., Phys. Rev. C 99 (2019) 021302, <https://doi.org/10.1103/PhysRevC.99.021302>.
- [8] B.S. Nara Singh, Z. Liu, R. Wadsworth, H. Grawe, T.S. Brock, et al., Phys. Rev. Lett. 107 (2011) 172502, <https://doi.org/10.1103/PhysRevLett.107.172502>.
- [9] K.P. Lieb, D. Kast, A. Jungclaus, I.P. Johnstone, G.d. Angelis, et al., Phys. Rev. C 63 (2001) 054304, <https://doi.org/10.1103/PhysRevC.63.054304>.
- [10] N. Boelaert, N. Smirnova, K. Heyde, J. Jolie, Phys. Rev. C 75 (2007) 014316, <https://doi.org/10.1103/PhysRevC.75.014316>.
- [11] N. Boelaert, A. Dewald, C. Fransen, J. Jolie, A. Linnemann, et al., Phys. Rev. C 75 (2007) 054311, <https://doi.org/10.1103/PhysRevC.75.054311>.
- [12] A. Corsi, A. Obertelli, P. Doornenbal, F. Nowacki, H. Sagawa, et al., Phys. Rev. C 97 (2018) 044321, <https://doi.org/10.1103/PhysRevC.97.044321>.
- [13] G.A. Müller, A. Jungclaus, O. Yordanov, E. Galindo, M. Hausmann, et al., Phys. Rev. C 64 (2001) 014305, <https://doi.org/10.1103/PhysRevC.64.014305>.
- [14] M. Siciliano, J.J. Valiente-Dobón, A. Goasduff, T.R. Rodríguez, D. Bazzacco, et al., Phys. Rev. C 104 (2021) 034320, <https://doi.org/10.1103/PhysRevC.104.034320>.
- [15] P.E. Garrett, T.R. Rodríguez, A.D. Varela, K.L. Green, J. Bangay, et al., Phys. Rev. Lett. 123 (2019) 142502, <https://doi.org/10.1103/PhysRevLett.123.142502>.
- [16] A.T. Schmidt, K.L.G. Heyde, J. Jolie, Phys. Rev. C 96 (2017) 014302, <https://doi.org/10.1103/PhysRevC.96.014302>.
- [17] M. Górška, M. Lipoglavšek, H. Grawe, J. Nyberg, A. Atač, et al., Phys. Rev. Lett. 79 (1997) 2415, <https://doi.org/10.1103/PhysRevLett.79.2415>.
- [18] A. Blazhev, M. Górška, H. Grawe, J. Nyberg, M. Palacz, et al., Phys. Rev. C 69 (2004) 064304, <https://doi.org/10.1103/PhysRevC.69.064304>.
- [19] A. Blazhev, N. Braun, H. Grawe, P. Boutachkov, B.S.N. Singh, et al., J. Phys. Conf. Ser. G 205 (2010) 012035, <https://doi.org/10.1088/1742-6596/205/1/012035>.
- [20] R.M. Clark, J.N. Wilson, D. Appelbe, M.P. Carpenter, C.J. Chiara, et al., Phys. Rev. C 61 (2000) 044311, <https://doi.org/10.1103/PhysRevC.61.044311>.
- [21] A. Ekström, J. Cederkäll, D.D. DiJulio, C. Fahlander, M. Hjorth-Jensen, et al., Phys. Rev. C 80 (2009) 054302, <https://doi.org/10.1103/PhysRevC.80.054302>.
- [22] B.A. Brown, K. Rykaczewski, Phys. Rev. C 50 (1994), <https://doi.org/10.1103/PhysRevC.50.R2270>, R2270(R).
- [23] G.d. Angelis, C. Fahlander, D. Vretenar, S. Brant, A. Gadea, et al., Phys. Rev. C 60 (1999) 014313, <https://doi.org/10.1103/PhysRevC.60.014313>.
- [24] P.E. Garrett, K.L. Green, H. Lehmann, J. Jolie, C.A. McGrath, et al., Phys. Rev. C 75 (2007) 054310, <https://doi.org/10.1103/PhysRevC.75.054310>.
- [25] M. Déléze, S. Drissi, J. Kern, P.A. Terrier, J.P. Vorlet, Nucl. Phys. A 551 (1993) 269, [https://doi.org/10.1016/0375-9474\(93\)90482-D](https://doi.org/10.1016/0375-9474(93)90482-D).
- [26] K. Heyde, C.D. Coster, J. Jolie, J.L. Wood, Phys. Rev. C 46 (1992) 541, <https://doi.org/10.1103/PhysRevC.46.2113>.
- [27] J. Jolie, H. Lehmann, Phys. Lett. B 342 (1) (1995), [https://doi.org/10.1016/0370-2693\(94\)01392-P](https://doi.org/10.1016/0370-2693(94)01392-P).
- [28] K. Heyde, J. Jolie, H. Lehmann, C.D. Coster, J.L. Wood, Nucl. Phys. A 586 (1) (1995), [https://doi.org/10.1016/0375-9474\(94\)00721-X](https://doi.org/10.1016/0375-9474(94)00721-X).
- [29] H. Lehmann, J. Jolie, Nucl. Phys. A 588 (1995) 623, [https://doi.org/10.1016/0375-9474\(95\)00045-3](https://doi.org/10.1016/0375-9474(95)00045-3).
- [30] C.D. Coster, K. Heyde, B. Decroix, P.V. Isacker, J. Jolie, et al., Nucl. Phys. A 600 (1996) 251, [https://doi.org/10.1016/0375-9474\(96\)00019-X](https://doi.org/10.1016/0375-9474(96)00019-X).
- [31] H. Lehmann, J. Jolie, C.D. Coster, B. Decroix, K. Heyde, et al., Nucl. Phys. A 621 (1997) 767, [https://doi.org/10.1016/S0375-9474\(97\)00196-6](https://doi.org/10.1016/S0375-9474(97)00196-6).
- [32] C.D. Coster, B. Decroix, K. Heyde, J. Jolie, H. Lehmann, et al., Nucl. Phys. A 621 (1997) 802, [https://doi.org/10.1016/S0375-9474\(97\)00195-4](https://doi.org/10.1016/S0375-9474(97)00195-4).
- [33] C.D. Coster, B. Decroix, K. Heyde, J. Jolie, H. Lehmann, et al., Nucl. Phys. A 651 (1999) 31, [https://doi.org/10.1016/S0375-9474\(99\)00124-4](https://doi.org/10.1016/S0375-9474(99)00124-4).
- [34] H. Geissel, P. Armbruster, K. Behr, A. Brünle, K. Burkard, et al., Nucl. Inst. Meth. B 70 (1) (1992) 286–297, [https://doi.org/10.1016/0168-583X\(92\)95944-M](https://doi.org/10.1016/0168-583X(92)95944-M).
- [35] A. Mistry, H. Albers, T. Arici, A. Banerjee, G. Benzoni, et al., Nucl. Inst. Meth. A 1033 (2022) 166662, <https://doi.org/10.1016/j.nima.2022.166662>.
- [36] O. Hall, T. Davinson, C. Griffin, P. Woods, C. Appleton, et al., Nucl. Inst. Meth. A 1050 (2023) 168166, <https://doi.org/10.1016/j.nima.2023.168166>.
- [37] J. Simpson, Z. Phys. A 358 (1997) 139–143, <https://doi.org/10.1007/s002180050290>.
- [38] M. Rudigier, Z. Podolyák, P. Regan, A. Bruce, S. Lalkovski, et al., Nucl. Inst. Meth. A 969 (2020) 163967, <https://doi.org/10.1016/j.nima.2020.163967>.
- [39] General machine timing system at GSI and FAIR <https://www-acc.gsi.de/wiki/Timing/WebHome>, 2021. (Accessed 20 October 2021).
- [40] M. Górška, R. Schubart, H. Grawe, J.B. Fitzgerald, D.B. Fossan, et al., Z. Phys. A 350 (1994) 181.
- [41] D. Alber, A. Berger, H.H. Bertschat, H. Grawe, H. Haas, et al., Z. Phys. A (ISSN 0939-7922) 344 (1) (1992) 1–11, <https://doi.org/10.1007/BF01291011>.
- [42] W.F. Piel, C.W. Beausang, D.B. Fossan, R. Ma, E.S. Paul, et al., Phys. Rev. C 37 (Mar 1988) 1067–1076, <https://doi.org/10.1103/PhysRevC.37.1067>.
- [43] J. Park, R. Krücken, D. Lubos, R. Gernhäuser, M. Lewitowicz, et al., Phys. Rev. C 96 (2017) 044311, <https://doi.org/10.1103/PhysRevC.96.044311>.
- [44] J.-M. Régis, H. Mach, G. Simpson, J. Jolie, G. Pascović, et al., Nucl. Inst. Meth. A 726 (2013) 191, <https://doi.org/10.1016/j.nima.2013.05.126>.
- [45] J.-M. Régis, J. Jolie, N. Saed-Samii, N. Warr, M. Pfeiffer, et al., Phys. Rev. C 95 (2017) 054319, <https://doi.org/10.1103/PhysRevC.95.054319>.
- [46] E. Gamba, A. Bruce, M. Rudigier, Nucl. Inst. Meth. A 928 (2019) 93–103, <https://doi.org/10.1016/j.nima.2019.03.028>.
- [47] T. Kibédi, T.W. Burrows, M.B. Trzhaskovskaya, P.M. Davidson, C.W. Nestor, Nucl. Inst. Meth. A 589 (2008) 202–229, <https://doi.org/10.1016/j.nima.2008.02.051>.
- [48] R.M. Pérez-Vidal, A. Gadea, C. Domingo-Pardo, A. Gargano, J.J. Valiente-Dobón, et al., Phys. Rev. Lett. 129 (2022) 112501, <https://doi.org/10.1103/PhysRevLett.129.112501>.
- [49] L. Coraggio, L. De Angelis, T. Fukui, A. Gargano, N. Itaco, et al., Phys. Rev. C 100 (2019) 014316, <https://doi.org/10.1103/PhysRevC.100.014316>.
- [50] K. Suzuki, R. Okamoto, Prog. Theor. Phys. 93 (1995) 905, <https://doi.org/10.1143/ptp/93.5.905>.
- [51] Data extracted using the NNDC On-line Data Service from the ENSDF database, file revised as of February 22, 2023.
- [52] L. Coraggio, N. Itaco, G. De Gregorio, A. Gargano, R. Mancino, et al., Phys. Rev. C 105 (2022) 034312, <https://doi.org/10.1103/PhysRevC.105.034312>.
- [53] T. Togashi, Y. Tsunoda, T. Otsuka, N. Shimizu, M. Honma, Phys. Rev. Lett. 121 (2018) 062501, <https://doi.org/10.1103/PhysRevLett.121.062501>.
- [54] L. Coraggio, A. Covello, A. Gargano, N. Itaco, T.T.S. Kuo, Phys. Rev. C 91 (2015) 041301, <https://doi.org/10.1103/PhysRevC.91.041301>.
- [55] L. Coraggio, A. Gargano, N. Itaco, Phys. Rev. C 93 (2016) 064328, <https://doi.org/10.1103/PhysRevC.93.064328>.
- [56] L. Coraggio, A. Gargano, N. Itaco, Phys. Rev. C 93 (2016) 064328, <https://doi.org/10.1103/PhysRevC.93.064328>.
- [57] L. Coraggio, A. Covello, A. Gargano, N. Itaco, T.T.S. Kuo, Phys. Rev. C 91 (2015) 041301, <https://doi.org/10.1103/PhysRevC.91.041301>.
- [58] N. Pietralla, P. von Brentano, A. Lisetskiy, Prog. Part. Nucl. Phys. 60 (1) (2008) 225–282, <https://doi.org/10.1016/j.pnpnp.2007.08.002>.
- [59] R. Casperson, V. Werner, S. Heinze, Phys. Lett. B (ISSN 0370-2693) 721 (1) (2013) 51–55, <https://doi.org/10.1016/j.physletb.2013.02.042>.